

CRITICAL HEAT FLUX MARGIN EVALUATION

Francisco Antonio Braz Filho

Institute for Advanced Studies (IEAv - CTA), São José dos Campos, SP, Brazil.
e-mail: fbraz@ieav.cta.br

Alexandre David Caldeira

Institute for Advanced Studies (IEAv - CTA), São José dos Campos, SP, Brazil.
e-mail: alexdc@ieav.cta.br

Eduardo Madeira Borges

Institute for Advanced Studies (IEAv - CTA), São José dos Campos, SP, Brazil.
e-mail: eduardo@ieav.cta.br

Abstract. An accurate calculation of the critical heat flux (CHF) margin is highly desirable, due to its utilization as a design parameter for various cooling and heating systems, such as pressurized water reactors (PWRs). In this work, the CHF margin was obtained through the direct substitution and the heat balance methods, using subcooled or low quality CHF correlations, without correction factors. Considering a simple heated channel and the direct substitution method, it is shown that the W-2, W-3 and EPRI correlations and look-up tables, used to predict CHF margins, may yield results strongly dependent on the adopted correlation. It is suggested that the application of the heat balance method to such correlations may be more appropriate. For the calculation, the CHF correlations were incorporated in a computer program called COTHA.

Keywords: critical heat flux, CHF correlations, DNB, boiling crisis, two-phase flow.

1. Introduction

An essential matter of reactor core design is the critical heat flux (CHF), that has also been called departure from nucleate boiling (DNB), and more recently, the boiling crisis (El-Wakil, 1978). The mechanism of boiling crisis differs in various flow patterns, as shown in Fig. (1). In subcooled or bubbly flow, the bubbly boundary layer flows parallel to the wall with a liquid core flowing at the center of the tube. A local void fraction peak is observed and measured near the wall. When the boundary layer separates from the wall, a stagnant fluid forms under the layer. Due to the heat flux at the surface, this stagnant fluid evaporates, resulting in a vapor blanket on the heated wall. When the wall temperature exceeds the Leidenfrost point, the boiling crisis occurs. Nucleate boiling usually prevails in a bubbly flow. The boiling heat transfer rate is reduced suddenly as the flow stagnation occurs. Hence, this type of boiling crisis is also called departure from nucleate boiling (Tong, 1967).

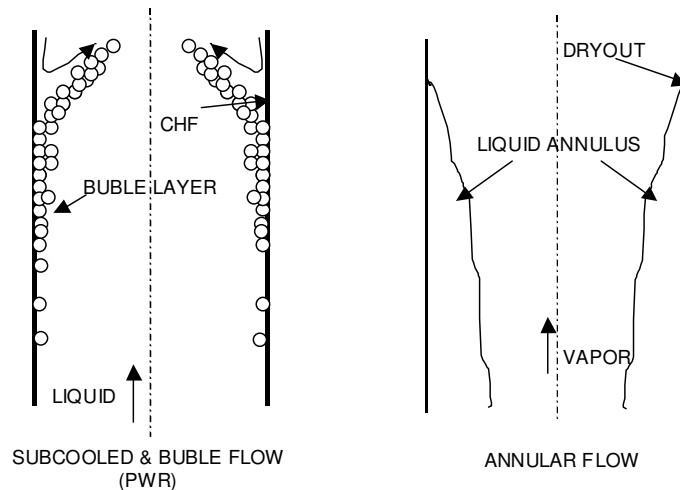


Figure 1. Boiling crisis mechanism in subcooled and annular flow.

The study of this phenomenon has applications in chemical, mechanical and nuclear industries, mainly in nuclear reactors and heat exchangers (boilers and condensers). This paper focuses on nuclear reactor core applications.

When CHF takes place, the consequences may be as follows: the surface may overheat and become damaged; corrosion in CHF region; and reduction in operating efficiency.

The major design limitation on the power capacity of a Pressurized Water Reactor (PWR) core, under normal operating conditions, is the CHF phenomenon, or DNB (Tong & Weisman, 1979). The safety margin incorporated in a nuclear reactor core thermal design necessarily limits the power capacity of the core. By increasing the DNB safety margin, we obviously increase the likelihood that there will be no failure, but decrease the power capacity. The most significant parameter is the minimum CHF ratio (CHFR) defined in the form:

$$\text{CHFR} = \frac{\text{CHF predicted by a correlation}}{\text{local heat flux}} \quad (1)$$

Among the various forms to predict CHF, one can mention: analytical models, empirical correlations and look-up tables. Analytical models (Chun et al, 2000) have more academic appeal, but are usually limited to a narrow range of conditions of data base for which the constitutive relations are measurable. There are more than five hundred available correlations for water flow inside tubes, but only three correlations are considered in this paper because of their importance for the nuclear community. They are the W-3 (Hsu & Graham, 1986), W-2 (Tong, 1967) and EPRI (Columbia University, 1983) correlations. CHF correlations are valid mainly within the range of their data bases and cannot be extrapolated to conditions far beyond those ranges, due to incorrect trends. To overcome this problem, Groeneveld et al (1986) proposed the CHF look-up tables, which was a significant improvement over the CHF correlation approach. An updated version of the look-up table for CHF was developed in 1996 by AECL (Canada) and IPPE (Russia) (Groeneveld et al, 1996). The look-up table for CHF has become a widely accepted prediction technique and has the following advantages over correlations: accurate prediction; widest ranges of applications; ease of use (no fluid properties are needed); ease of updating; and correct parametric and asymptotic trends.

As it was already mentioned, an accurate calculation of the critical heat flux (CHF) margin is highly desirable, due to its utilization as a design parameter for various cooling and heating systems. In this work, the critical heat flux margin is obtained through the application of two major existing methods: the Direct Substitution Method (DSM) and the Heat Balance Method (HBM), using subcooled or low quality CHF correlations and look-up tables. Considering a simple heated channel and the direct substitution method, it is shown that the W-3, W-2, EPRI and look-up tables correlations, used to predict CHF margins, may yield results strongly dependent on the adopted correlation. This suggests that the application of the heat balance method to such correlations may be more appropriate. The purpose of this paper is to discuss these results, to provide an integrated explanation of the potential problems in using and interpreting correlation results and to evaluate the mentioned correlations.

Inasaka & Nariai (1996) clearly showed in a theoretical work that, for subcooled flow boiling CHF, HBM always gives predictions closer to the actual value, with respect to DSM. The same researchers also verified this result experimentally. In their paper, all correlations used to predict CHFR gave better predictions of experimental data when using HBM rather than DSM. Hejzlar and Todreas (1996) argued that the application of the HBM to such correlations, which leads to an expression for the CHF margin in terms of critical power ratio, may be more appropriate than DSM. Groeneveld et al (1996) found a much better performance of their look-up tables when using HBM rather than DSM. Celata (1996) has a stronger opinion. He believes HBM is the only correct method for applications in CHF correlations. However, Siman-Tov (1996) takes the opposite position. According to Siman-Tov's view, only DSM is correct for comparison of correlation with experimental data because DSM involves the comparison of the CHF correlation predicted to experimental heat flux, under the same thermo-hydraulic conditions, while HBM compares heat fluxes at different thermo-hydraulic conditions.

This paper contains the description of correlations types, the demonstration of the two methods (DSM and HBM) to calculate the CHF margin, discussion of the results and conclusions.

2. Correlations

As in Hejzlar & Todreas (1996), the present work separates the correlations for the subcooled or low quality region in two groups. The type 1 CHF correlation has the form:

$$q''_{\text{CHF}} = f(G, x, p, D_h), \quad (2)$$

or if the effect of heated length L is taken into account:

$$q''_{\text{CHF}} = f(G, x, p, D_h, L), \quad (3)$$

where G is the mass flux, p is the pressure, D_h is the channel hydraulic diameter and x is the cross-sectional average thermodynamic quality. Typical examples of these correlations are the look-up tables.

If the local quality x is eliminated by incorporating the heat balance along the channel up to the point z of interest, the type 2 CHF correlation is originated and takes the form:

$$q''_{CHF} = f\left(G, x_{in} \text{ or } h_{in}, p, D_h, z \text{ or } \frac{x - x_{in}}{q''}\right). \quad (4)$$

A typical example of the type 2 correlation with the $(x - x_{in})/q''$ class parameter is the EPRI correlation.

If the last term in Eq. (4) is z , it is very important to note that this distance must appear as a residual of a term $(x - x_{in})/q''$, i.e., it must satisfy the heat balance equation since this ratio can be readily rewritten using heat balance to yield pure z dependence (Hejzlar & Todreas, 1996). This will be clarified when the representation of operating conditions through the energy balance is derived. An important characteristic of both the $(x - x_{in})/q''$ term and the z term is their independence on the channel power. This can be observed from the latter term, since both terms $(x - x_{in})$ and q'' are directly proportional to power level, hence their ratio does not depend on channel power.

There are some hybrid correlations, which make an attempt to take into account upstream condition effects by introducing an inlet condition variable (x_{in} or h_{in}) but do not incorporate a full heat balance. Some correlations also account for the heated length effects by incorporating the distance parameter, mostly in the form of a z/D_h ratio. These correlations have both the inlet and the local conditions as parameters, i.e.,

$$q''_{CHF} = f\left(G, x_{in} \text{ or } h_{in}, p, D_h \text{ or } \frac{z}{D_h}, x\right). \quad (5)$$

This correlation type will be further designated as a semilocal correlation of type 1, since its behavior is similar to that of this type. Typical examples are the W-3 and W-2 correlations.

Typical CHF behavior predicted by the correlation types is sketched in $q'' \times z$ and $q'' \times x$ coordinates illustrated in Fig. (2) for the fixed parameters G, D_h, x_{in} , and p . The CHF curves are assumed to have a negative slope since CHF typically decreases as the equilibrium quality increases. To show the two different correlation types in one sketch, type 2 correlation is assumed to give slightly lower values of CHF than the type 1 correlation. Note that for increasing channel power, the type 1 correlation in $q'' \times z$ space yields reduced CHF while the type 2 correlation has identical curves for various channel powers. This is because with increasing channel power the quality parameter in the correlation of the type 1 increases, while the type 2 correlation is independent on x . In the $q'' \times x$ coordinates, where the quality x represents in fact the critical quality for various operating channel powers, the type 1 correlation exhibits dependence on x (CHF is typically decreasing with increasing x) while the type 2 correlation exhibits zero partial derivative relative to x parameter, i.e., it yields the same CHF for all x .

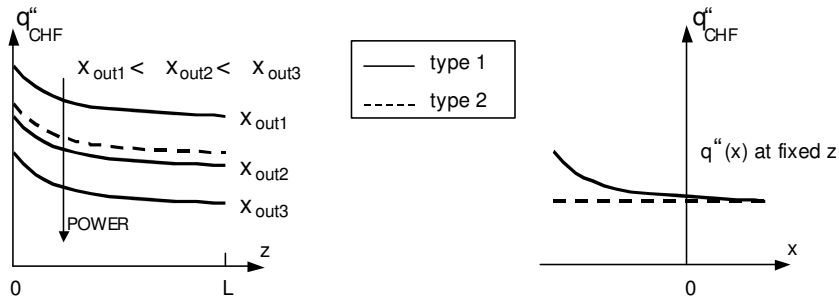


Figure 2. A sketch of CHF correlation types in different coordinate systems.

3. Methods to calculate the CHF margin

The two methods generally used to calculate CHF margins along the channel are the Direct Substitution Method (DSM) and the Heat Balance Method (HBM).

For understanding these methods, a simple heated round tube will be considered. It is assumed a channel of length L and hydraulic diameter D_h , with the walls heated by an axially non-uniform heat flux, $q''(z)$. The channel operates at the total power:

$$\dot{Q} = \pi D_h \int_0^L q''(z) dz = P_h \int_0^L q''(z) dz, \quad (6)$$

where P_h is the heated perimeter.

Channel operating conditions at various axial positions can be represented in two graphs as shown schematically in Fig. (3). The left-hand graph shows the sketch of the operating heat flux as a function of axial coordinate z . As the channel power increases, the operating heat flux, as well as the quality, increases. Note that the flux shape is assumed to be independent on the power, i.e., an increase in channel power does not result in a change in the normalized axial flux profile.

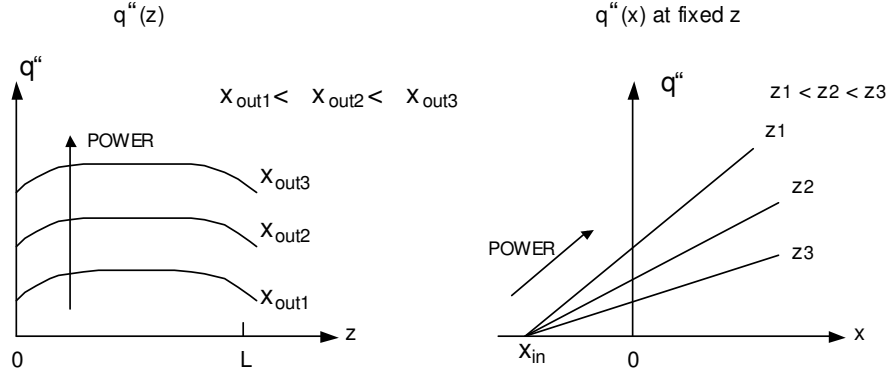


Figure 3. Representation of heat flux for various channel powers.

An alternative way of representing the operating condition is in $q'' \times x$ coordinates. The right-hand side of Fig. (3) shows the operating heat flux at three selected fixed axial positions from the channel inlet up to the position of interest. The local quality can be represented by:

$$x = x_{in} + \frac{P_h}{G A h_{fg}} \int_0^z q''(\bar{z}) d\bar{z} , \quad (7)$$

where A is the channel flow area, h_{fg} is the enthalpy difference between vapor and liquid and z is z_1 , z_2 or z_3 for the curves presented in Fig. (3). The differing slopes of these curves follow from the relative locations of z_1 , z_2 and z_3 on the flux profile shown. This slope, for a fixed position z , can be calculated by rewriting Eq. (7) with the use of the non-uniformity flux factor $F(z)$ as:

$$q''(z) = \frac{x - x_{in}}{F(z) P_h z} G A h_{fg} , \quad (8)$$

where:

$$F(z) = \frac{1}{q''(z) z} \int_0^z q''(\bar{z}) d\bar{z} \quad (9)$$

is the ratio between the average heat flux from the channel inlet to the coordinate z of the interest and the local channel heat flux at this location. Equation (8), for fixed $z = z_1$, can be rewritten in function of the quality as:

$$q''(x) = \frac{G A h_{fg}}{F(z_1) P_h z_1} x - \frac{G A h_{fg}}{F(z_1) P_h z_1} x_{in} , \quad (10)$$

which is a linear function and the slope is given by:

$$\frac{G A h_{fg}}{F(z_1) P_h z_1} . \quad (11)$$

Figure (4) shows both the operating conditions of the channel, Eq. (11), and the CHF curve, Eq. (2), at a fixed axial location z in $q'' \times x$ coordinates. For the operating heat flux q''_{oper} , the local quality x corresponding to this heat flux, at a fixed location z , can be seen in the heat balance curve as the OP point. The CHF curve represents generally any CHF correlation type with negative slope.

The purpose of this work is to calculate the CHF margin at various axial positions of the channel, i.e., $CHFR(z)$ or $DNBR(z)$. This will be done with the DSM and HBM methods.

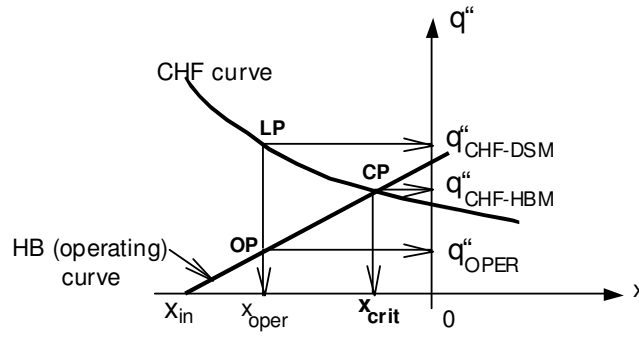


Figure 4. Heat balance (operating conditions) and CHF curves.

For DSM, the local quality at each position of interest, x_{oper} , can be calculated using the heat balance and the operating heat flux q''_{oper} ; this local quality is then directly substituted into the CHF correlation to obtain q''_{CHF_DSM} . Thus, $CHFR_{DSM}$ is calculated as:

$$CHFR_{DSM} = \frac{q''_{CHF_DSM}}{q''_{oper}} . \quad (12)$$

An alternative designation for DSM is “local condition approach”, since CHF is found from the local quality x_{oper} , i.e., using the local quality directly in the CHF correlation (point LP in the CHF curve). In practice, in the thermo-hydraulic design of PWRs, DSM has been used most often, since it is simple and does not require any iteration.

For HBM, q''_{CHF_HBM} at axial location z is calculated by varying the magnitude of the heat flux input into the channel, i.e., increasing the channel power and preserving the flux shape, until the critical heat flux given by the CHF correlation at this location is reached, i.e., a channel heat flux which achieves exactly critical conditions at the point z of interest is found. In other words, one is looking for the intersection of the heat balance curve and the CHF curve, denoted in Fig. (4) as point CP (critical point). $CHFR_{HBM}$ is calculated as:

$$CHFR_{HBM} = \frac{q''_{CHF_HBM}}{q''_{oper}} . \quad (13)$$

CHFR determined by HBM can be designated as the critical heat flux power ratio (CHFPR), since for an isolated subchannel it is equal to the critical power ratio (CPR). To find the intersection of the CHF curve and the heat balance curve for type 1 correlations, an iterative process is necessary. One practical way to find the solution is to combine the heat balance, Eq. (8), and the CHF correlation, Eq. (2), in the form:

$$\frac{x - x_{in}}{F(z)P_h z} G A h_{fg} - f(G, x, p, D_h) = 0 , \quad (14)$$

which can be solved for the quality x . The quality which satisfies the Eq. (14) is the critical quality, x_{crit} , that corresponds to the critical heat flux, q''_{CHF_HBM} . Another possible approach is to increase successively the channel power until critical conditions at a location of interest are reached. This yields the heat flux corresponding to the critical channel power q''_{CHF_HBM} , which can be substituted into Eq. (13) to obtain CHFPR. The former method is applicable only to isolated subchannels where the energy balance is valid, while the latter (the usual approach for obtaining a CPR) is applicable also to rod bundles (as in nuclear reactors), provided that a subchannel code, such as COBRA (Wheeler et al, 1976), which can treat cross flow between individual subchannels is available.

Note that no iterative method is necessary for type 2 correlations, which effectively employ Eq. (14) as part of the correlation, in this case $q''_{CHF_HBM} = q''_{CHF_DSM}$.

The sketch in Fig. (4) illustrates that CHFR calculated by the direct substitution approach may be higher than that obtained by the heat balance approach. The magnitude of the difference depends on the correlation. If the slope of the CHF correlation in $q'' \times x$ space is small, the difference is small, and vice-versa.

Note that for type 1 correlations, at a location of interest, the more the operation quality, x_{oper} , approximates the critical quality, the more the critical heat flux calculated by DSM, q''_{CHF_DSM} , approximates the critical heat flux calculated by HBM, q''_{CHF_HBM} .

For the calculation, the mentioned correlations and related methods were incorporated in a computer program called COTHA (Braz Filho et al, 2002).

4. Discussion of results

To compare the described methods, DSM and HBM, and to evaluate the correlations without correction factors, two samples cases will be used. In both cases, the geometry considered is a round pipe with 8 mm of diameter and uniform heat flux. This diameter dimension and geometry are chosen because the 1996 CHF look-up table (Groeneveld et al, 1996) data are normalized for 8 mm round tube. This CHF look-up table is considered as one of the best and widely used prediction methods, and for which statistics (average and root mean square errors of 0.69% and 7.82%, respectively), based on HBM, are available. The following parameters were adopted for the *case a*: heat flux of 1.5 MW m^{-2} , mass flux of $5000 \text{ kg s}^{-1} \text{ m}^{-2}$, pressure of 10 MPa and inlet subcooling (thermodynamic quality) of -0.273 . For the *case b*, the parameters are: heat flux of 3.5 MW m^{-2} , mass flux of $5000 \text{ kg s}^{-1} \text{ m}^{-2}$, pressure of 16 MPa and inlet subcooling of -0.850 . Only results obtained within the recommended range of the correlations are considered.

Figures (5) and (6) show the CHF margin (CHFR) calculated along the channel, using DSM and HBM for W-3, W-2 and EPRI correlations and look-up tables (1986 and 1996 versions), with regard to the *cases a* and *b*, respectively. Figure (6) presents both methods using all correlations and look-up tables. It is important to note that all results converge to CHFR equal to one, at the point located at the channel output. This occurs because all the correlations represent, within their uncertainty, measured data, which were obtained at critical conditions and also, as discussed, both methods converge to the same CHF at this point (CP). Figures (5) and (6) show that for type 1 correlations (W-3 and W-2 correlations and look-up tables) DSM always yields much higher values than HBM.

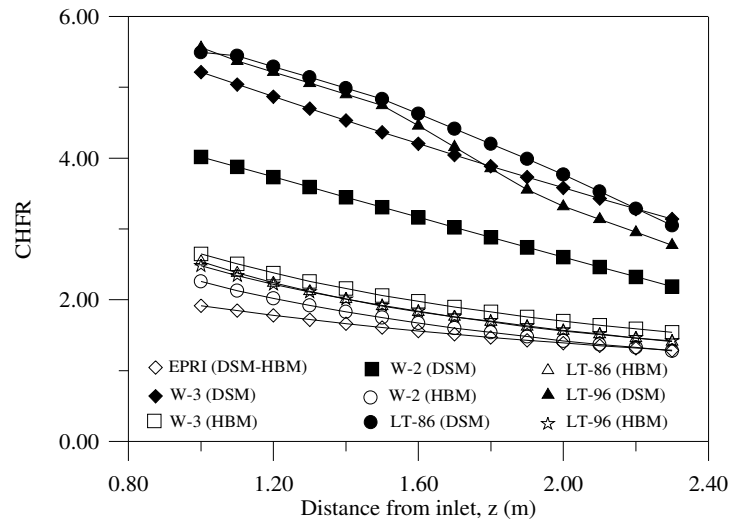


Figure 5. Comparison of the DSM and HBM methods (*case a*).

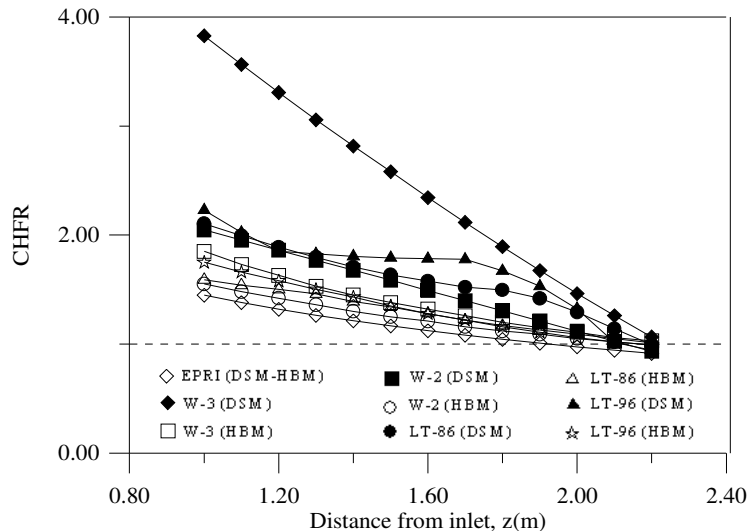


Figure 6. Comparison of the DSM and HBM methods (*case b*).

Figures (7) and (8) present CHF_R along the channel, using only DSM, for all the correlations and look-up tables, with respect to the cases *a* and *b*, respectively. The curves are rather different from each other, i.e., the results are strongly dependent on the correlation adopted.

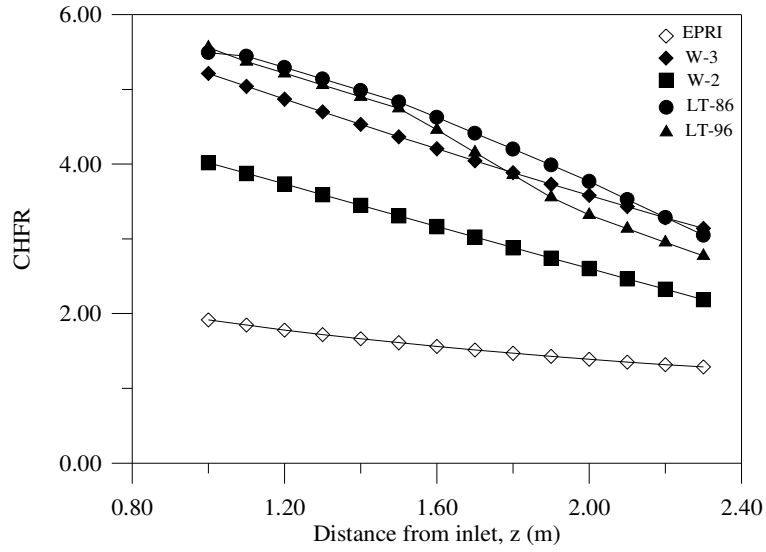


Figure 7. CHF_R along the channel, using DSM (*case a*).

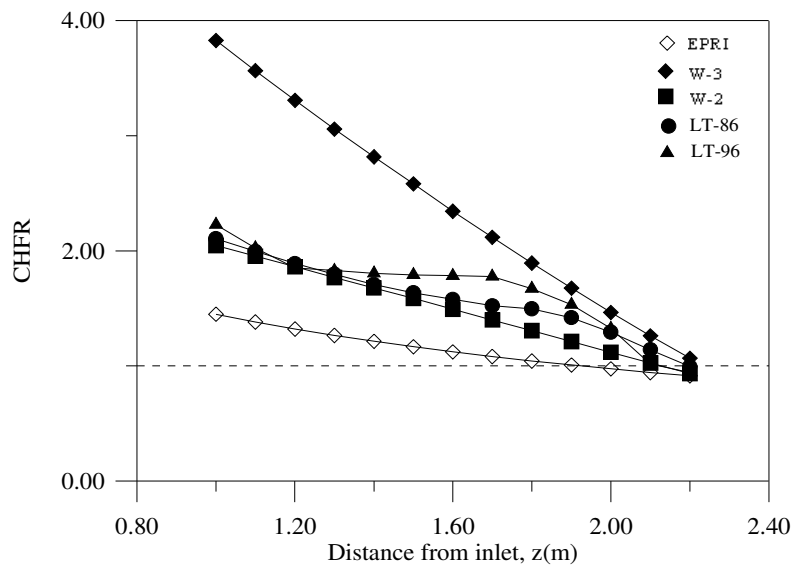


Figure 8. CHF_R along the channel, using DSM (*case b*).

Figures (9) and (10) present CHFR along the channel, using only HBM, for all the correlations and look-up tables, with respect to the *cases a* and *b*, respectively. The curves are much closer than in the previous graphs.

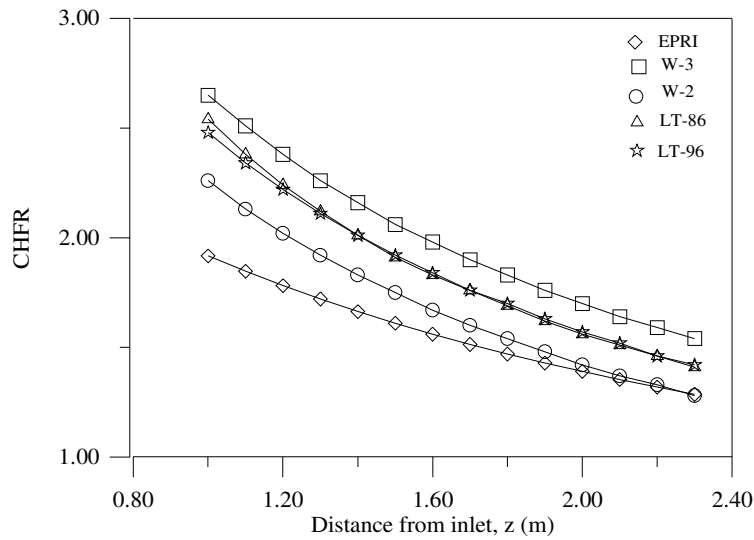


Figure 9. CHFR along the channel, using HBM (*case a*).

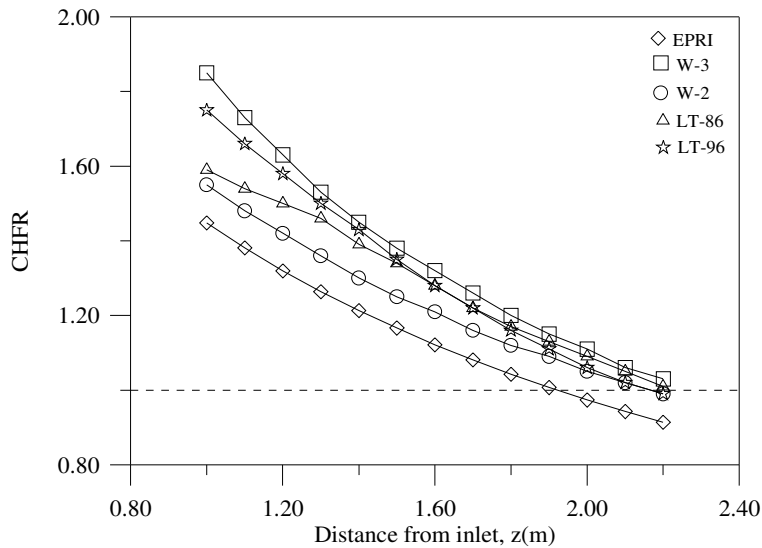


Figure 10. CHFR along the channel, using HBM (*case b*).

Table (1) presents percent errors for all correlations and look-up tables, using both methods (DSM and HBM), with respect to the data obtained from the look-up table (1996) using HBM (*case b*) that is considered the best result by the literature. Two points were chosen to compare these data: $CHFR=1.28$ and $CHFR=1.35$, that are the points closer to the value 1.3, adopted for design of PWRs. As can be seen, the data obtained, using DSM, for type 1 correlation are very discrepant while for HBM the results are better in agreement. In addition, Tab. (1) also presents, to the same conditions, percent errors at the point $CHFR=1$. At this point, all results are in a reasonable agreement and the differences obtained are due to the correlation's precision.

Table 1. Percent errors for all correlations and look-up tables, using both methods DSM and HBM, with respect to the data obtained from the 1996 look-up table (LT), using HBM (*case b*).

Correlation (method)	Error (%)		
	CHFR=1.35	CHFR=1.28	CHFR=1.0
EPRI (DSM & HBM)	14	12	8
W-3 (DSM)	-91	-83	-8
W-3 (HBM)	-2	-3	-4
W-2 (DSM)	-17	-16	6
W-2 (HBM)	7	6	0
LT-1986 (DSM)	-21	-23	0
LT-1986 (HBM)	1	0	-2
LT-1996 (DSM)	-32	-39	5
LT-1996 (HBM)	0	0	0

Figures (11) and (12) present $q''_{CHF-DSM} \times x$, for fixed z (channel output), for all the correlations and look-up tables, with respect to the *cases a* and *b*, respectively. As can be observed, the curves are rather different from each other for $CHFR \gg 1$ and approximate when $CHFR=1$. These figures show also the heat balance curve. For type 2 correlations, as EPRI, the curve is a horizontal line because it is not dependent on the quality.

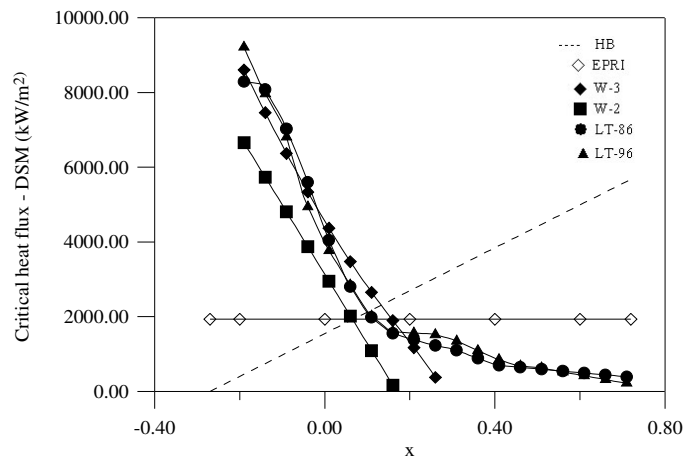


Figure 11. CHF as a function of the quality for all correlations and look-up tables, using DSM (*case a*).

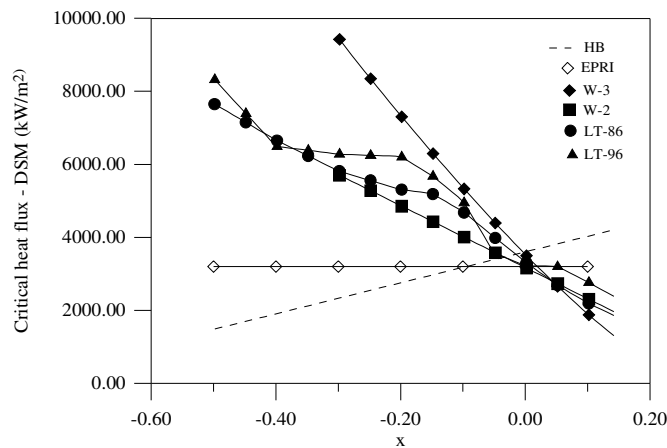


Figure 12. CHF as a function of the quality for all correlations and look-up tables, using DSM (*case b*).

5. Conclusions

Correlations and look-up tables were utilized to predict the CHF margin, without their correction factors that take into account various effects such as channel length, diameter, non-uniformity of axial heat flux, heated diameter, etc.

Furthermore, it was analyzed the simplest case that can be treated using look-up tables, and for which statistics (average and root mean square errors) are available. This approach was made on purpose, because application of correction factors and other influences could mask the results. In the future, new analyses that also consider correction factors will be necessary.

The correlations were divided in two classes (type 1 and 2) and two methods were approached (DSM and HBM).

Normally, to CHF margin evaluation, DSM is incorporated in codes for thermo-hydraulic analysis of nuclear reactors, mainly because it is the most simple method and it does not required any iteration. For rod bundles, such as in nuclear reactors, where radial mixing takes place, the heat balance described by the Eq. (7) cannot be done. Moreover, CHFPR also depends on the cross flow which itself may be power level dependent. To calculate CHF_{HBM} it is necessary to increase successively the channel power until critical conditions at a location of interest are reached to find the heat flux corresponding to critical channel power, which, divided by the operating heat flux, yields CHFPR. Thus, the application of HBM can be problematic in this situation, because the codes used must be executed many times. HBM should not be used in fast transients where the time-dependent fluctuation of any correlation parameter is comparable to the transport time of the coolant on the channel. Hence, the use of HBM is limited to steady state or quasi-steady-state analysis. It can be observed that in some cases there are local hot spots or hot stripes, where the heat flux can be locally high and cause localized CHF without affecting significantly the global heat balance or local thermo-hydraulic conditions. Such cases also need the application of DSM.

CHF type 1 correlations, as the look-up tables, W-3 and W-2, yield much higher values using DSM than when using HBM. Moreover, the CHFR value obtained with this correlation type using DSM depends strongly on the correlation adopted. As shown before, when CHFR is approximately 1.0, the results is in reasonable agreement with the look-up table results using HBM; when CHFR moves away from 1.0, results become much higher than those of the look-up table results using HBM. Thus, when correlations of type 1 and DSM are used, the results obtained must be understood as a relative value, i.e., it must be established a CHF margin specifically for this situation, that is dependent on the selected correlation.

CHF type 2 correlations, which incorporate a full heat balance, give a CHFR equal to CHFPR. Therefore the traditional DSM can always be applied to obtain CHFR or CHFPR from such correlations. The CHF margin calculated from type 2 correlations, as EPRI, using DSM, showed reasonable agreement with those of the look-up table using HBM and the results always yielded conservative values.

The results obtained with the CHF type 1 correlations, as W-3, W-2 and the 1986 look-up table, using HBM, had good agreement with the 1996 look-up table using HBM and it is suggested that, whenever possible, this correlation type be used together with this method.

6. References

- Braz Filho, F. A. et al, 2002, "Um Programa Computacional para Análise Termoidráulica de Núcleos de Reatores do Tipo Placa", XIII ENFIR, Rio de Janeiro, Brazil, 2002.
- Celata, G. P., 1996, "On the Application Method of Critical Heat Flux Correlations", Nuclear Engineering and Design, Vol. 163, pp. 241-242.
- Chun T. H. et al, 2000, "An Integral Equation Model for Critical Heat Flux at Subcooled and Low Quality Flow Boiling", Nuclear Engineering and Design, Vol. 199, pp. 13-29.
- Columbia University, 1983, "Parametric Study of CHF Data – Volume 2: A Generalized SubChannel CHF Correlation for PWR and BWR Fuel Assemblies", EPRI NP-2609, Vol. 2, New York, USA.
- El-Wakil, M. M., 1978, "Nuclear Heat Transport", ANS, Illinois, USA.
- Groeneveld, D. C. et al, 1986, "AECL-UO Critical Heat Flux Look-up Table", Heat Transfer Engineering, Vol. 7, pp. 46-62.
- Groeneveld, D. C. et al, 1996, "The 1995 Look-up Table for Critical Heat Flux in Tubes", Nuclear Engineering and Design, Vol. 163, pp. 1-23.
- Hejzlar, P. & Todreas N. E., 1996, "Consideration of Heat Flux Margin Prediction by Subcooled or Low Quality Critical Heat Flux Correlations", Nuclear Engineering and Design, Vol. 163, pp. 215-223.
- Hsu, Y. Y. & Graham, R. W., 1986, "Transport Processes in Boiling and Two-phase Systems", ANS, Illinois, USA.
- Inasaka, F. & Nariai, H., 1996, "Evaluation of Subcooled Critical Heat Flux Correlations for Tubes with and without Interval Twisted Tapes", Nuclear Engineering and Design, Vol. 163, pp. 225-239.
- Siman-Tov, M., 1996, "Technical Note: Application of Energy Balance and Direct Substitution Methods for Thermal Margin and Data Evaluation". Nucl. Eng. Des., Vol. 163, pp. 249-258.
- Tong, L. S., 1967, "Heat Transfer in Water Cooled Nuclear Reactors", Nuclear Engineering and Design, Vol. 6, pp. 301-324.
- Tong, L. S. & Weisman, J., 1979, "Thermal Analysis of Pressurized Water Reactors", ANS, Illinois, USA.
- Wheeler, C. L. et al, 1976, "COBRA-IV-I: An Interim Version of COBRA for Thermal-Hydraulic Analysis of Rod Bundle Nuclear Fuel Elements and Cores", BNWL-1962 UC-32, Battelle, Pacific Northwest Laboratories, Richland, USA.